

This is a repository copy of *Computational electromagnetic (CEM) model validation against measured and calculated results*.

White Rose Research Online URL for this paper:

<https://eprints.whiterose.ac.uk/180108/>

Version: Accepted Version

---

**Proceedings Paper:**

Dawson, J F [orcid.org/0000-0003-4537-9977](https://orcid.org/0000-0003-4537-9977), Robinson, M P [orcid.org/0000-0003-1767-5541](https://orcid.org/0000-0003-1767-5541) and Konefal, T (2004) Computational electromagnetic (CEM) model validation against measured and calculated results. In: Validation of Computational Electromagnetics, IEE Seminar on , 17-21 , March 2004. , pp. 17-24.

<https://doi.org/10.1049/ic:20040105>

---

**Reuse**

Items deposited in White Rose Research Online are protected by copyright, with all rights reserved unless indicated otherwise. They may be downloaded and/or printed for private study, or other acts as permitted by national copyright laws. The publisher or other rights holders may allow further reproduction and re-use of the full text version. This is indicated by the licence information on the White Rose Research Online record for the item.

**Takedown**

If you consider content in White Rose Research Online to be in breach of UK law, please notify us by emailing [eprints@whiterose.ac.uk](mailto:eprints@whiterose.ac.uk) including the URL of the record and the reason for the withdrawal request.

## COMPUTATIONAL ELECTROMAGNETIC (CEM) MODEL VALIDATION AGAINST MEASURED AND CALCULATED RESULTS

J F Dawson, M P Robinson and T Konefal

University of York, UK

### INTRODUCTION

The Applied Electromagnetics Research Group at the University of York are both users and developers of numerical electromagnetic codes. CEM codes are used extensively to allow us to determine field data which is impractical or impossible to measure, also to optimise the design of electromagnetic systems. However the "art" of numerical electromagnetic modelling is to produce a model which is simple enough to compute, yet containing the essential detail required to accurately model the real physical system. In order to validate the model, measured or analytical results are used. The first challenge is to find a system which can be both modelled and measured accurately. The second is to discover where the error lies when the result disagree! The third is deciding which model result most accurately fits the measured data.

The paper presents examples of the validation of numerical models using measured and calculated results from a range of research projects undertaken at York. These aim to show that both the measurement and computational model are approximate representations of the real-world, and that significant effort must be made to ensure that they are sufficiently similar if useful results and validation are to be obtained. We shall also discuss how the choice of metrics for the comparison of numerical, analytical and measured data is influenced by the nature of the EM problem being investigated

### MODEL VALIDATION

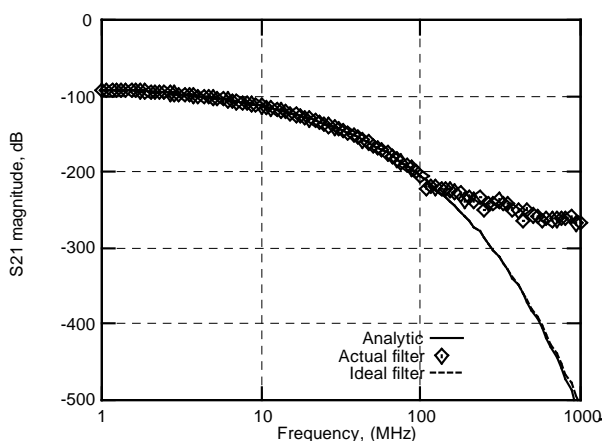


Figure 1: Transmission Through 5mm thick 30kS/m conducting sheet, Analytic, ideal, and actual model).

### Validation with analytic solution

The simplest solution to the problem of validating a numerical model occurs when an analytic solution also exists. There is no need to consider any uncertainty associated with measurement. The development of a thin conducting layer model for our TLM code is a good example of this (1).

#### Transmission through a thin conducting layer.

Figure 1 shows a comparison of the analytic solution, an ideal model and the actual implementation. The effect of finite precision of the (32bit floating point) implementation can be seen as the transmission coefficient ceases to fall as it meets the numerical noise floor.

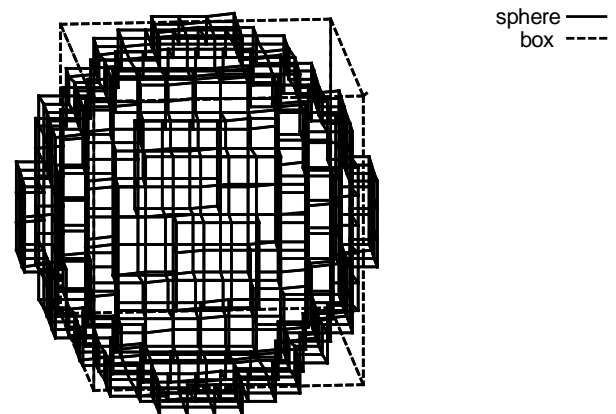


Figure 2: 3-D Validation geometry for the thin conducting layer model.

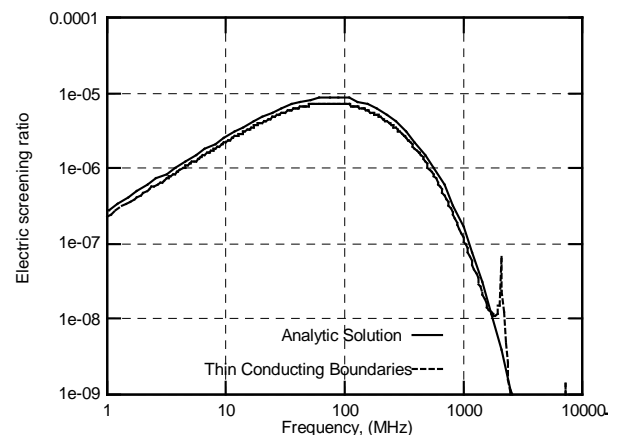


Figure 3: Electric field screening ratio for sphere – TLM simulation with thin conducting boundary model compared with analytic solution.

Figure 2 shows a 3-D TLM model of a spherical shell constructed from the thin conducting layer model. Figure 3 shows the electric field screening ratio predicted by the model and an analytic solution (1). The analytic solution here does not account for the (real) resonance which can be seen in the model.

### Model validation against measurement

Most of the numerical modelling carried out in the York research group undergoes comparison with measured data in order to validate the model. The main difficulty encountered here is developing a scenario which can be both measured and modelled accurately. A typical example is shown below.

**Radiated emissions from a heatsink.** The sample heatsink has many fins. Due to the complexity of modelling the full details we opted to model a simpler geometry Figure 4.

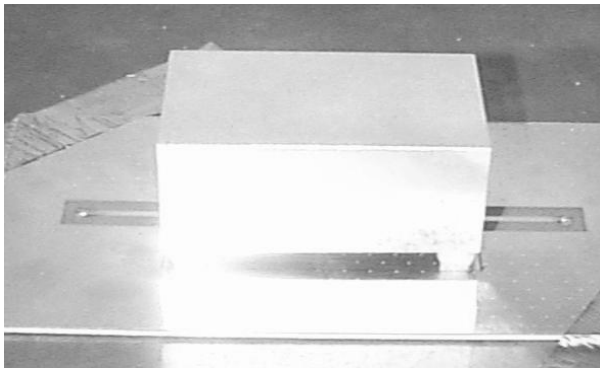


Figure 4: The solid block heatsink used for comparison with the numerical models

In order to allow validation of the numerical model the set-up shown in Figure 5 was used for both measurements and the computational model. The heatsink was supported at each corner by a small dielectric support (not included in the numerical model) over a ground plane. The centre of the heatsink was fed by a 50Ω source via a short wire (0.7 mm diameter) protruding from the ground plane. This is similar to the common mode excitation due to voltage drops in the leads of an IC package and can also be easily produced in the laboratory to allow validation of the model by measurement. A 3cm high monopole at 1 m from the centre of the heatsink, connected to a 50Ω load was used to sense the radiated field for model validation purposes.

Microwave absorber was placed around the edges of the ground plane to limit the effect of reflections from nearby objects, as the measurements were carried out on a laboratory bench. Measurements were performed using a network analyser to determine the transmission from heatsink to monopole (S21). The connecting cables to the heatsink and antenna were underneath the ground plane and so did not interact with the measurement.

In the model an ideal infinite ground plane was used, the absorber and cables were not included.

The use of an OATS or anechoic chamber, with a Bi-log type antenna might well be the obvious choice for many engineers when presented with this problem. The reason for our chosen setup was entirely due to the fact that we could model the entire system (almost).

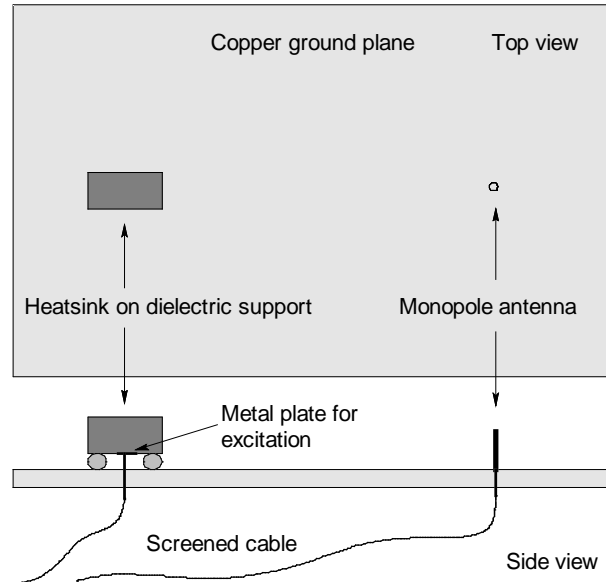


Figure 5: Measurement set-up for validation of numerical models

Figure 6 shows one example of the coupling between the heatsink and small antenna. The measurement noise floor is also shown – it is very easy to think you have data when all you measure is noise.

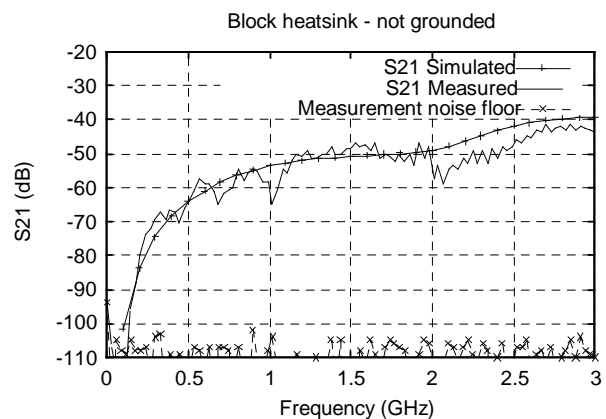


Figure 6: Comparing the measured and simulated S21 from heatsink feed to monopole base for the block heatsink - not grounded.

As we were interested in the effect of grounding the heatsink, Figure 7 shows the ratio of coupling measured with no grounding to that measured with the heatsink grounded at each corner. Again the measurement noise floor is shown, and accounts for the deviation between measured and simulated results at low frequencies.

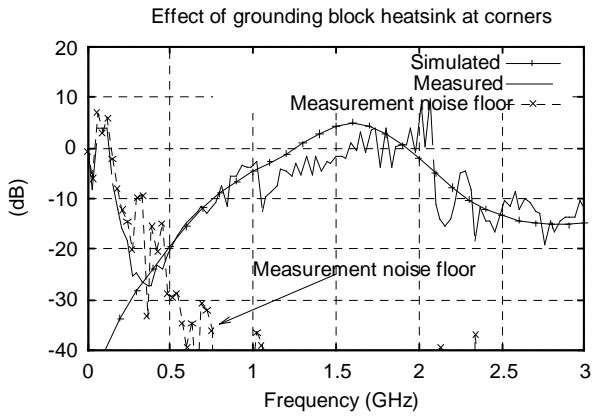


Figure 7: Comparing the measured and simulated effect of grounding just the corners of the block heatsink (Power grounded / Power not grounded).

### COMPARISON OF DATA

We now consider the role of data comparison in the validation of CEM models. Subjective expressions such as ‘poor agreement’ or ‘excellent agreement’ are widely used in the literature but a numerical metric is clearly more desirable. In EMC applications we often have to consider the frequency variation of a quantity such as shielding effectiveness (SE) or radiated field. The simplest metrics for comparing such data sets are not necessarily the most appropriate.

Frequency responses in EMC problems often show a number of resonances, which occur when structures such as enclosures and cables are electrically large. The peaks of these resonances are important because that is when the greatest amount of energy is entering or leaving an electronic system and potentially causing EMI. The Q-factor is also very significant as it is closely related to the electromagnetic losses in a system, although its importance often receives too little attention in the literature.

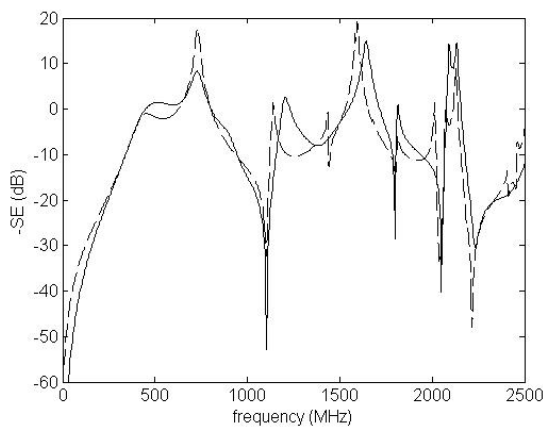


Figure 8: plot of SE for ‘TLM’ (solid) and ‘ILCM’ (dashed)

An example is shown in Figure 8, which shows the SE of an enclosure calculated by the transmission line

matrix (TLM) method and by a much faster intermediate level computer model (ILCM). The vertical axis shows  $-SE$  to emphasise the resonant peaks. Most EMC experts would say that these curves show good agreement: the plots run close together in the smoothly varying response at low frequency, and the resonant features above 500MHz occur at approximately the right frequencies.

A common way of comparing curves is to consider the differences at each frequency, and calculate either the mean absolute error (MAE) or mean square error (MSE). The problem with applying such metrics to EMC data is that small offsets in peak frequency can generate large values of MAE or MSE. We have generated three artificial data sets to illustrate this point. (Figure 9 and Figure 10). Which is closer to A: B or C?

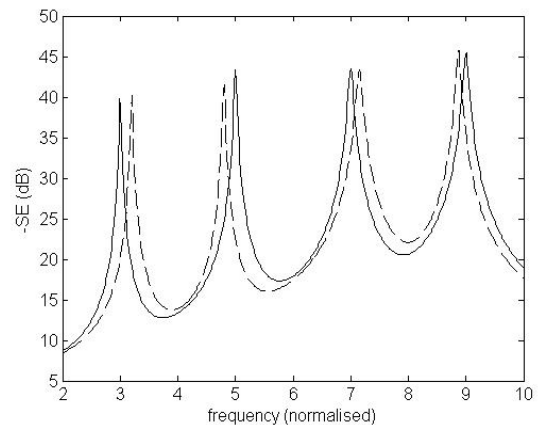


Figure 9 11: data sets ‘A’ (solid) and ‘B’ (dashed)

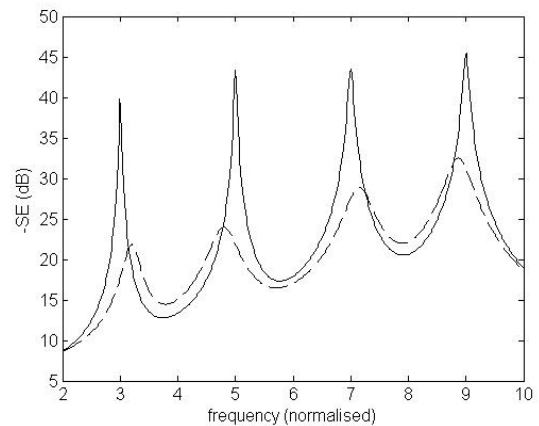


Figure 10: data sets ‘A’ (solid) and ‘C’ (dashed)

We can see ‘by eye’ that AB is a better match than AC. The peaks are slightly offset but in fact the peaks in C are at the same frequencies as those in B. In C the trend is approximately correct but the peak values are wrong by 15-20dB which would be very poor for EMC modelling. However if we try to use metrics such as MSE to compare the curves the results are counter-intuitive. In Table 1 we present the mean absolute error and root-mean-square (rms) error on both logarithmic (decibel) and linear scales.

TABLE 1 – comparison of data sets using four different metrics

| metric                       | A and B           | A and C           |
|------------------------------|-------------------|-------------------|
| mean absolute error (dB)     | 3.7               | 3.2               |
| rms error (dB)               | 5.4               | 4.9               |
| mean absolute error (linear) | $1.7 \times 10^3$ | $1.1 \times 10^3$ |
| rms error (linear)           | $5.1 \times 10^3$ | $4.0 \times 10^3$ |

All four metrics actually give AC as closer to AB. The problem is that these metrics only consider ‘vertical’ errors, but what we have is large vertical errors but only small horizontal errors. It is not just a simple frequency shift because some peak offsets are positive and others negative.

### Alternative methods

An alternative method is to extract parameters that characterise the peaks, and compare these rather than the raw data. We have written a program that finds the peak frequency  $f_p$ , Q-factor and peak power for each resonance, by applying a curve-fitting algorithm to the points near the maxima in the frequency response (3).

The peak parameters for data sets A, B, C are shown in Figure 11 and Figure 12. We can see that the distance between equivalent points is much less for AB than for AC. If we normalise the values of  $f_p$  and Q to the range of the axes in Figure 11 and Figure 12, then the average Euclidean distance between equivalent points is 0.067 for AB but 0.68 for AC. So an average distance in ‘fQ’ space might be a better metric than MEA or MSE. The method could be extended by also including peak power for a distance in 3-d ‘fQP’ space.

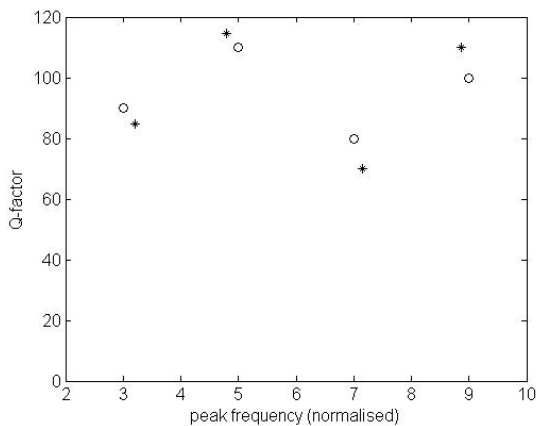


Figure 11: comparison of peak parameters for data sets ‘A’ (circles) and ‘B’ (stars)

There are two problems with this metric. First, how to choose appropriate scales for the f, Q and P axes? Secondly, what to do if there are different numbers of peaks in the data sets? CEM models may sometimes produce extra or missing peaks. An example is given

by Figure 13, which shows the peak parameters for the raw data in Figure 8. The first four pairs of points can be easily matched but at frequencies above 2000MHz it becomes more difficult. Spurious peaks may also be caused by measurement noise, so it is important to have a knowledge of the noise floor of the instrumentation, as highlighted above. Dealing with these problems is an ongoing area of our research.

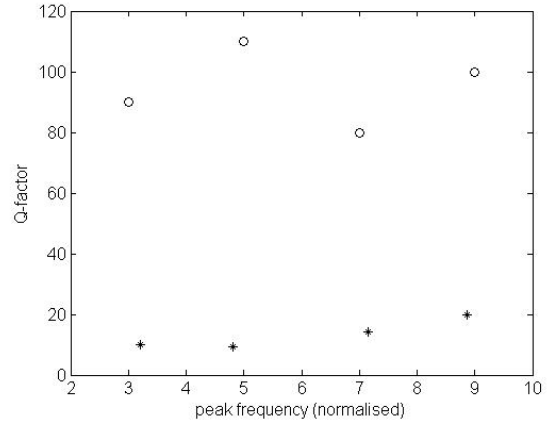


Figure 12: comparison of peak parameters for data sets ‘A’ (circles) and ‘C’ (stars)

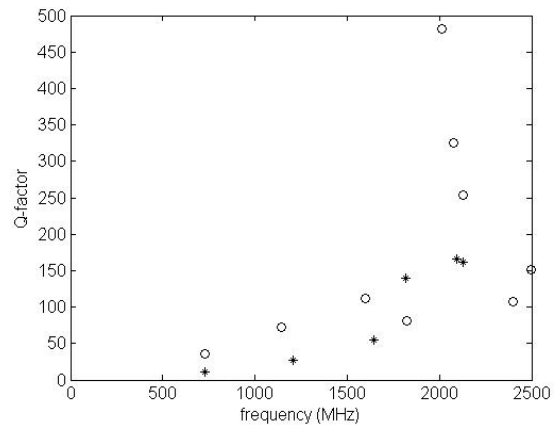


Figure 13: comparison of peak parameters for SE data obtained by ‘TLM’ (circles) and ‘ILCM’ (stars)

A number of alternative methods have been considered by Weissenfeld (4) as part of a study into an innovative shielding measurement. One of these draws inspiration from dynamic time warping (DTW) which is a technique used for matching of audio data (5). The algorithm involves expanding or compressing parts of the horizontal axis in order to match up the resonant peaks, and then calculating the mean square difference. The result is two metrics: an average frequency shift and an ‘improved’ MSE. Initial results have been encouraging, although this algorithm also has problems dealing with different numbers of peaks in the two data sets.

These alternative methods offer the possibility of a more appropriate metric than MAE or MSE, although they are clearly less straightforward to apply.

## Statistical comparisons

When enclosures and other structures are electrically very large, then the mode density can become so great that hundreds or thousands of resonances contribute to the overall frequency response. An example is given by Figure 14, which shows  $-SE$  for an enclosure that is much larger than that of Figure 8. As the mode density increases, the exact frequency of each peak becomes very sensitive to small changes in the geometry of the enclosure, and so attempting to validate such a model against other data by MSE or peak-parameter comparison would be difficult.

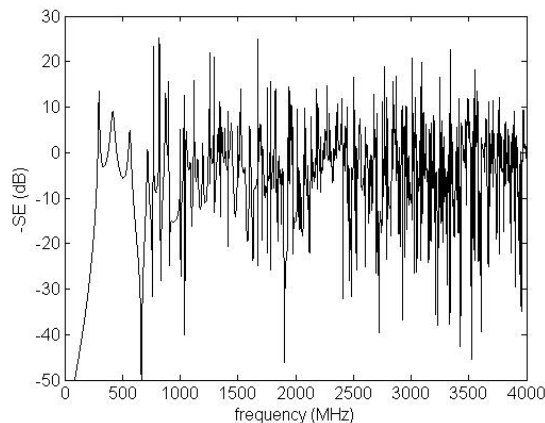


Figure 14: plot of SE calculated by TLM for a large enclosure, showing a greater mode density at higher frequencies

A alternative approach is to consider the statistical distribution of the quantity being modelled. If a sufficient number of modes is excited, the values of one component of the E-field at random positions in an enclosure, e.g  $E_y$ , should follow the Rayleigh distribution. An interesting question is how many modes are needed for this to be true. We have found by Monte-Carlo modelling that a key parameter  $\alpha$  is the ratio of the mode density (i.e. modes per Hz) to the average bandwidth of each mode. Figure 15 shows that as  $\alpha$  increases, the shape of the probability density function becomes closer to that of a perfect Rayleigh distribution.

It would be useful to have a single number to describe how closely the distribution resembles the ideal for a multi-mode enclosure. We have found that a suitable metric here is the ratio of mean to standard deviation which is 1.06 for a single mode in a rectangular cavity, and 1.91 for the Rayleigh distribution. Table 2 shows how this ratio quantifies the shift in the distribution as the mode density increases.

## CONCLUSIONS

Gaining measurement data against which to validate numerical models requires careful attention to detail to ensure that the two systems are identical. The best method of comparing data sets depends on the nature

of the data being compared. Mean square error may be a good metric for slowly varying frequency responses, while for resonant responses alternative methods such as peak-parameter comparison may be more suitable. For very high mode densities statistical parameters would be most appropriate.

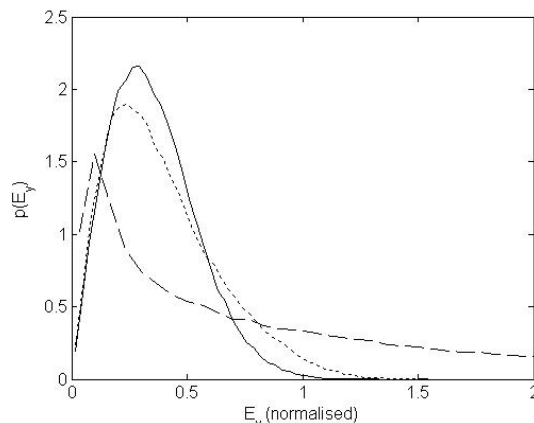


Figure 15: probability density functions for  $\alpha=30$  (solid),  $\alpha=1$  (dotted) and  $\alpha=0.1$  (dashed)

TABLE 2 – ratio of mean of  $E_y$  to standard deviation of  $E_y$  for different values of  $\alpha$

| $\alpha$ | ratio of mean to standard deviation |
|----------|-------------------------------------|
| 0.1      | 1.09                                |
| 1        | 1.55                                |
| 30       | 1.90                                |

## ACKNOWLEDGEMENTS

The authors gratefully acknowledge the support of BAE Systems, Sun Microsystems, and QinetiQ who have supported parts of the work reported here.

## REFERENCES

1. Cole, J. A., Dawson, J. F., Porter S. J., 1996, "Efficient Modelling of Thin Conducting Sheets within the TLM method", IEE 3rd Int. Conference on Computation in Electromagnetics, Bath, 10-12 April , pp45-50
2. Dawson, J. F., Marvin, A. C., Porter, S. J., Nothofer, A., Will, J. E., Hopkins, S., 2001, "The effect of grounding on radiated emissions from heatsinks", IEEE International symposium on EMC, Montreal, 13-17 Aug pp. 1248-1252
3. Robinson, M. P., Clegg, J., Stone D A, 2003. "A novel method of studying total body water content using a resonant cavity: experiments and numerical simulation" *Phys. Med. Biol.* **48** pp 113-125
4. Weissenfeld, A., 2003, "New type of shielding measurement for equipment enclosures" Studienarbeit Thesis, University of Hanover
5. Keogh, E. J., Pazzani, M. J. 1999, "Scaling up Dynamic Time Warping to Massive Datasets", Principles and Practice of Knowledge Discovery in Databases, Prague, Czech Republic